The dietary isothiocyanate sulforaphane targets pathways of apoptosis, cell cycle arrest, and oxidative stress in human pancreatic cancer cells and inhibits tumor growth in severe combined immunodeficient mice

Nhu-An Pham,[1,2] James W. Jacobberger,[3] Aaron D. Schimmer,[1,2] Pinjiang Cao,[2] Marcella Gronda,[2] and David W. Hedley[1,2]

[1]Department of Medical Biophysics, University of Toronto, Toronto, Ontario, Canada; [2]Ontario Cancer Institute, Princess Margaret Hospital, Toronto, Ontario, Canada; and [3]Comprehensive Cancer Center, Case Western Reserve University, Cleveland, Ohio

Abstract

Anticancer effects of the dietary isothiocyanate sulforaphane were investigated in the human pancreatic cancer cell lines MIA PaCa-2 and PANC-1. Sulforaphane-treated cells accumulated in metaphase as determined by flow cytometry [4C DNA content, cyclin A(−), cyclin B1(+), and phospho-histone H3 (Ser^{10})(+)]. In addition, treated cells showed nuclear apoptotic morphology that coincided with an activation of caspase-8, loss of mitochondrial membrane potential, and loss of plasma membrane integrity. The initial detection of caspase-3 cleavage occurring in G_2-M arrest was independent of a change in phospho-cdc2 (Tyr^{15}) protein; consequently, sulforaphane treatment combined with UCN-01 had no significant impact on cellular toxicity. Incubations at higher sulforaphane doses (>10 μmol/L) resulted in cleavage of caspase-3 in the G_1 subpopulation, suggesting that the induction of apoptosis and the sulforaphane-induced mitosis delay at the lower dose are independently regulated. Cellular toxicity in MIA PaCa-2, and to a greater extent in PANC-1, was positively correlated with a decrease in cellular glutathione levels, whereas sustained increases in glutathione observed in MIA PaCa-2 cells or the simultaneous incubation with *N*-acetyl-L-cysteine in PANC-1 cells were associated with resistance to sulforaphane-induced apoptosis. Daily sulforaphane i.p. injections (375 μmol/kg/d for 3 weeks) in severe combined immunodeficient mice with PANC-1 s.c. tumors resulted in a decrease of mean tumor volume by 40% compared with vehicle-treated controls. Our findings suggest that, in addition to the known effects on cancer prevention, sulforaphane may have activity in established pancreatic cancer. [Mol Cancer Ther 2004; 3(10):1239–48]

Introduction

Isothiocyanates are components of certain plants and vegetables that have selective biological activities and functions against carcinogenesis (1). Sulforaphane, a potent cancer preventive agent, is a dietary isothiocyanate compound found as a precursor glucosinolate in cruciferous vegetables such as cauliflower, broccoli, and Brussels sprouts (2). Epidemiologic and clinical studies reviewed by Murillo and colleagues indicate a positive correlation between the general consumption of cruciferous vegetables and the decreased incidence of some cancers including non-Hodgkin's lymphoma, liver, prostate, cervical, ovarian, lung, and gastrointestinal tract (3–6). Oral administration of sulforaphane inhibited or retarded experimental multistage carcinogenesis models including cancers of the breast (7), colon (8, 9), stomach (10), and lung (11). Previously, these anticancer effects were attributed to modulation of carcinogen metabolism by the inhibition of metabolic activation of phase I enzymes and the induction of phase II detoxification enzymes and glutathione (GSH) levels (12, 13).

Subsequently, several independent mechanisms seemed to play significant roles in the prevention of cancer development including the activation of c-Jun NH_2-terminal kinase (14) and extracellular signal-regulated kinase-1/2 (15), interaction with redox-sensitive proteins (16–18), and induction of cell cycle arrest (19, 20). The antiproliferative effects of isothiocyanates on cancer cells have been associated with detected changes of various cell cycle regulators [e.g., cyclin A and cyclin B1 (21) and cdk1, cdc25B, and cdc25C (22)]. The use of naturally occurring compounds combined with chemotherapy might enhance drug sensitivity (23). The development of such novel approaches for pancreatic cancer treatment is essential as tumor cells are highly resistant to conventional chemotherapy drugs.

Effects of sulforaphane and the synthetic alkyl isothiocyanates on two established pancreatic cell lines MIA PaCa-2 and PANC-1, which contain mutant p53 and activated *ras* (24–26), were investigated in this study. In agreement with previously reported observations on effects of

Received 2/10/04; revised 8/11/04; accepted 8/20/04.

Grant support: National Cancer Institute of Canada, Graduate Scholarships Doctoral Award funded by Canada Institutes of Health Research (N-A. Pham), and Canadian Institute of Health Research Clinician Scientist (A.D. Schimmer).

The costs of publication of this article were defrayed in part by the payment of page charges. This article must therefore be hereby marked advertisement in accordance with 18 U.S.C. Section 1734 solely to indicate this fact.

Requests for reprints: David W. Hedley, Division of Experimental Therapeutics, Department of Medical Oncology and Hematology, Ontario Cancer Institute, Princess Margaret Hospital, 610 University Avenue, Toronto, Ontario, Canada M5G 2M9. Phone: 416-946-2262; Fax: 416-946-6546. E-mail: david.hedley@uhn.on.ca

isothiocyanates (19, 21, 22, 27), a G_2-M arrest was observed in the sulforaphane-treated pancreatic cancer cells. However, on further investigation, our data suggest a more complex mechanism involving cell cycle deregulation, apoptosis, and an oxidative stress pathway that seems to reflect differences in degree of sulforaphane-induced toxicity between the cell lines.

Materials and Methods

Chemicals and Reagents

Sulforaphane [1-isothiocyanato-(4*R*,S)-(methylsulfinyl)-butane], phenylbutyl isothiocyanate, and phenylpropyl isothiocyanate were obtained from LKT Laboratories (St. Paul, MN). UCN-01 (7-hydroxystaurosporine) was obtained from the Cancer Treatment Evaluation Program of the National Cancer Institute (Bethesda, MD). The antioxidant *N*-acetyl-L-cysteine was obtained from Sigma-Aldrich Canada Ltd. (Oakville, Ontario, Canada) and the general caspase inhibitor Z-Val-Ala-Asp(OMe)-CH_2F (zVAD.fmk) was obtained from Enzyme Systems Products (Livermore, CA). Fluorescent probes, carboxydichlorofluorescein diacetate, monobromobimane, 4′,6-diamidino-2-phenylindole, Hoechst 33342, propidium iodide, and 1,1′,3,3,3′,3′-hexamethylindodicarbocyanine were obtained from Molecular Probes (Eugene, OR). Antibodies to cleaved caspase-3, phospho-cdc2 (Tyr^{15}), and cdc2 were obtained from Cell Signaling Technologies, Inc. (Beverly, MA), and a FITC conjugated to cyclin B1 antibody was obtained from BD Biosciences PharMingen (San Diego, CA). A phycoerythrin-conjugated anti–cyclin A antibody was the gift of Dr. T. Vincent Shankey (Beckman-Coulter, Miami, FL). Rabbit polyclonal anti–phospho-histone H3 (Ser^{10}) (pH3) was obtained from Upstate (Lake Placid, NY). Secondary antibodies, goat anti-rabbit Alexa Fluor 647 and 488, were obtained from Molecular Probes.

Cell Culture

Human pancreatic ductal adenocarcinoma cell lines MIA PaCa-2 and PANC-1 were obtained from American Type Culture Collection (Rockville, MD) and grown as instructed in the product information sheets. The growth media were supplemented with 10% fetal bovine serum (CanSera, Rexdale, Ontario, Canada), and in addition, the growth medium for MIA PaCa-2 was supplemented with 2.5% horse serum (Invitrogen, Carlsbad, CA). Cell cultures were grown at 37°C in a humidified atmosphere containing 5% CO_2 and 95% filtered air.

During exponential growth phase, cells were incubated continuously with the test agents in 5 cm^2 dishes (Nunclon, Nalge Nunc International, Rochester, NY). A Coulter Z1 particle counter (Beckman-Coulter, Fullerton, CA) was used to count cell suspensions from the harvested adherent cells.

Flow Cytometry for Intracellular Staining

Mitochondrial Membrane Potential and Propidium Iodide. As described previously by Ng et al. (28), the mitochondrial membrane potential (MMP) in cells was detected by staining with 40 nmol/L 1,1′,3,3,3′,3′-hexamethylindodicarbocyanine and plasma membrane integrity was detected by staining with 1 μmol/L propidium iodide. Cells were harvested (1×10^6 cells/mL) and stained with 1,1′,3,3,3′,3′-hexamethylindodicarbocyanine at 37°C for 30 minutes and propidium iodide was added in the last 5 minutes of the incubation.

Cell Cycle Analysis. Cells were harvested and resuspended in PBS, permeabilized in 0.1% Triton X-100, and stained with 1 μg/mL 4′,6-diamidino-2-phenylindole for 30 minutes. The Multicycle software version 2.5 (Phoenix Flow Systems, San Diego, CA) was used for cell cycle analysis.

Measures of Cellular Reactive Oxygen Intermediate and GSH. Flow cytometry–based measurements of cellular content of reactive oxygen intermediates with carboxydichlorofluorescein diacetate and reduced GSH with monobromobimane were done as described previously (29). Cells were stained with 5 μmol/L carboxydichlorofluorescein diacetate in growth medium at 37°C for 30 minutes and 40 μmol/L monobromobimane was added in the last 5 minutes of the incubation. Simultaneously, cells were stained with the protocol MMP and propidium iodide to identify viable cells and assess their reactive oxygen intermediate and GSH levels.

Intracellular Antigen Staining. Aliquots of 1×10^6 cells were collected and resuspended in 100 μL of ice-cold PBS. The permeabilization and fixation of cells was achieved by the addition of methanol (stored at −20°C) to a final dilution of 90% and incubated 30 minutes on ice. Cells were washed twice with 2.5% bovine albumin in PBS (wash buffer) and incubated on ice for 30 minutes with 50 μL of the diluted primary antibody in wash buffer. When a fluorophore-conjugated secondary antibody labeling was required, cells were then washed twice with wash buffer and resuspended in 50 μL of 100× diluted secondary antibody for 30 minutes on ice. Prior to flow cytometry analysis, antibody-labeled cells were resuspended in fresh wash buffer and stained with 1 μg/mL 4′,6-diamidino-2-phenylindole for 30 minutes. Cell cycle proteins were assayed by incubating simultaneously with FITC-anti–cyclin B1, phycoerythrin-anti–cyclin A, and pH3 at 1 μg per 10^6 cells followed by the secondary labeling for detection of pH3 with anti-rabbit Alexa Fluor 647 (30). Apoptosis detection was by probing with anti-cleaved caspase-3 at 1 μg per 10^6 cells followed by labeling with anti-rabbit Alexa Fluor 488.

Flow Cytometry Setup

Cells were analyzed using an Epics Elite flow cytometer (Beckman-Coulter, Miami, FL) equipped with an air-cooled argon laser (20 mW) emitting at 488 nm, a HeNe laser (23 mW) emitting at 633 nm, and a water-cooled UV laser (15 mW). The HeNe and UV lasers were spatially separated by a 40 ms delay from the argon laser for the assays: MMP and propidium iodide, cleaved caspase-3, and reactive oxygen intermediate and GSH. The HeNe was colinear with the argon laser for analysis of cell cycle proteins. Fluorescent signals from the argon laser excitation were collected by filters: 610 ± 20 nm for propidium iodide; 525 ± 10 nm for Alexa Fluor 488, FITC, and carboxydichlorofluorescein

diacetate; and 575 ± 10 nm for phycoerythrin. Excitation of 1,1′,3,3,3′,3′-hexamethylindodicarbocyanine and Alexa Fluor 647 was by the HeNe laser and fluorescence emission was collected through a 675 ± 20 nm filter. Emission signals of 4′,6-diamidino-2-phenylindole-DNA complex and monobromobimane by UV laser excitation were collected through a 440 ± 20 nm filter.

Western Blot Analysis

Total protein extract of cells at subconfluent growth was prepared by incubation for 15 minutes on ice with an ice-cold hypotonic HEPES buffer (50 mmol/L, pH 8) containing 10% glycerol, 1% Triton X-100, 150 mmol/L NaCl, 1 mmol/L EDTA, 1.5 mmol/L $MgCl_2$, 100 mmol/L NaF, $Na_4P_2O_7 \cdot H_2O$, 0.1 mmol/L sodium orthovanadate, and protease inhibitors (Complete, Mini, Roche, Mannheim, Germany). Protein samples of an equal amount were denatured with 1 volume of 6× SDS sample buffer and loaded on a 12.5% SDS-PAGE. Electrophoresis was done under 200 mV for 50 minutes and nitrocellulose membrane transfer was done under 100 mV for 60 minutes (Mini Trans-Blot Cell, Bio-Rad Laboratories, Hercules, CA). Blots were blocked for 60 minutes at room temperature with 5% nonfat milk powder and 0.1% Tween 20 in PBS and exposed overnight at 4°C to a primary antibody against cdc2 (1:1,000 v/v), phospho-cdc2 (1:500 v/v), rabbit anti-human caspase-8 (1:1,000 v/v), or rabbit anti-human caspase-3 (1:1,000 v/v). Antibodies against caspase-8 and caspase-3 were gifts from Dr. J.C. Reed (La Jolla, CA). Blots were washed with PBS and 0.1% Tween 20 for 5 minutes (three times) and exposed for 60 minutes at room temperature to horseradish peroxidase–linked anti-rabbit Ig (Amersham Biosciences Ltd., Buckinghamshire, United Kingdom). Complexes of the primary and secondary antibodies were visualized using enhanced chemiluminescence (Amersham Biosciences) or SuperSignal West Pico Chemiluminescent (Pierce Biotechnology, Rockford, IL).

Morphologic Assessment of Nuclear Morphology and MMP

Cells were grown on Lab-Tek chamber slides (Nalge Nunc International) overnight and then incubated with the test agents. For microscopy examination, cells were stained *in situ* with a DNA probe, 1 μmol/L Hoechst, at room temperature for 5 minutes and nuclei were observed with a RTM-3 imaging system (Richardson Technologies, Inc., Bolton, Ontario, Canada). A 50 mW mercury lamp source was used when operating in the epifluorescence microscopy mode using appropriate excitation-emission filter cubes.

Tumor Xenograft Animal Model

Experiments were done on male severe combined immunodeficient mice (Ontario Cancer Institute, Toronto, Ontario, Canada) according to the regulation of the Canadian Council on Animal Care. PANC-1 tumors for implantation were initially grown from injections of PANC-1 cells (400 μL of 3×10^6 cells) at the s.c. abdomen site. A tumor piece of 3 to 4 mm in diameter was implanted at the same site into an experimental animal at the age of 6 weeks. After 17 days of tumor establishment in severe combined immunodeficient mice, at the start of exponential tumor growth phase, animals were randomly divided into the treatment groups (n = 8). Each animal received by i.p. injection (<300 μL) either PBS (vehicle control) or sulforaphane daily, excluding weekends, for 3 weeks. Sulforaphane dosing was initially at 250 μmol/kg body weight and increased to 375 μmol/kg body weight by the end of the second week. Animal body weight and tumor size were measured with a microcaliper and recorded every other day. Tumor volume was calculated using the formula: length × width^2 × 0.5236 (31).

Statistical Analysis

Results are expressed as mean ± SE. Treatment effects were compared using Student's t test and differences between means were considered to be significant when $P \leq 0.05$. Experiments were repeated at least three times.

Results

Sulforaphane Suppressed Growth and Triggered Activation of Caspase-3- and Caspase-8-Dependent Cell Death

Decreased growth rate of MIA PaCa-2 and PANC-1 cells with continuous sulforaphane incubation was initially observed in MIA PaCa-2 cells at 5 μmol/L sulforaphane (Fig. 1A). Both cell lines were inhibited from proliferation to the same extent when incubated with 10 μmol/L

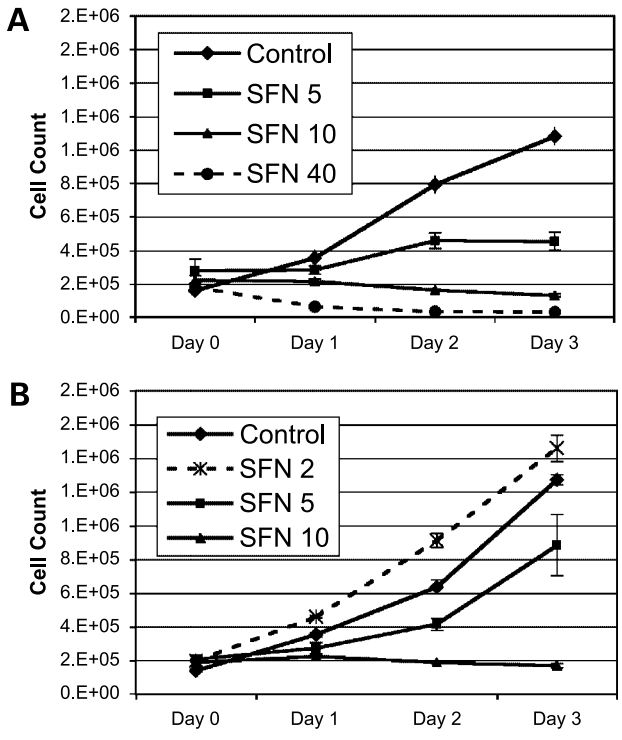

Figure 1. Dose-dependent inhibition of MIA PaCa-2 (**A**) and PANC-1 (**B**) cell growth during 3 days of continuous sulforaphane (*SFN*) exposure. Resistance to sulforaphane-induced toxicity was greater for MIA PaCa-2 than PANC-1, with adherent MIA PaCa-2 cells remaining after 40 μmol/L sulforaphane incubation.

sulforaphane. Almost total loss of adherent cells occurred when PANC-1 cells were treated at a dose higher than 10 μmol/L sulforaphane; thus, cell counts were not recorded (Fig. 1B).

To determine whether cell death was involved in growth suppression, cytotoxic effects of sulforaphane and two synthetic derivatives phenylpropyl isothiocyanate and phenylbutyl isothiocyanate were examined by flow cytometry. Viable cells were identified by the simultaneous measurement of MMP and the presence of an intact plasma membrane (Fig. 2A, *boxed region*). Initial cell damage was indicated by the loss of MMP while maintaining a relatively intact plasma membrane relative to the subpopulation of viable cells and progressing to the loss of plasma membrane integrity, indicating irreversible cell damage. Percentage of cell survival was equal when MIA PaCa-2 and PANC-1 cells were treated at 40 and 5 μmol/L sulforaphane, respectively, with continuous exposure for 24 hours (Fig. 2B and D). Cell viability analysis by flow cytometry from three independent experiments (Fig. 2E) shows that PANC-1 cells (*white bar*) were more sensitive to sulforaphane than MIA PaCa-2 cells (*black bar*). In contrast, no toxic effects were observed when cells were incubated with the synthetic analogues phenylpropyl isothiocyanate and phenylbutyl isothiocyanate at 10 and 100 μmol/L for up to 48 hours (Fig. 2F).

To substantiate these results, MIA PaCa-2 cells were assayed for caspase-3 cleavage. Dual staining in MIA PaCa-2 cells for cleaved caspase-3 and DNA content showed a low percentage of cleaved caspase-3-positive cells at 4C DNA content after 24-hour incubation with 10 μmol/L sulforaphane (Fig. 3B, *circled region*). However, when cells were incubated with 40 μmol/L sulforaphane, caspase-3 cleavage occurred primarily in G_1 (Fig. 3C, *circled region*). Consistent with the flow cytometry data, the microscopic examination of MIA PaCa-2 cells incubated with 10 μmol/L sulforaphane did not reveal extensive apoptosis. However, we did observe an accumulation of cells with mitotic nuclei (Fig. 3E) compared with control cells (Fig. 3D). More apoptotic nuclei were observed by microscopy when MIA PaCa-2 cells were incubated at the higher sulforaphane dose (Fig. 3F).

The two major pathways for caspase activation are the death receptor and mitochondrial pathways (32). We observed that treatment of PANC-1 cells with sulforaphane induced loss of procaspase-8 and increase of the cleaved form, consistent with activated caspase-8 and the death receptor pathway (Fig. 4). Activated caspase-8 occurred prior to the activation of caspase-3 as observed by the loss of procaspase-3 (Fig. 4B). Activation of caspase-8 also coincided with loss of MMP (Fig. 2), consistent with known amplification loop of the caspase pathways, confirming that sulforaphane acts within the death receptor pathway of caspase activation.

Perturbed Cell Cycle Regulation Unaffected by UCN-01

In addition to apoptotic effects, we evaluated effects on the cell cycle. Flow cytometric cell cycle analysis showed an accumulation of cells at 4C DNA content for MIA PaCa-2 (Fig. 5B) and PANC-1 (Fig. 5E), being more prominent in MIA PaCa-2 than in PANC-1 cells. This block was not apparent at 40 μmol/L sulforaphane in either cell line (Fig. 5C and F). Thus, cell growth suppression at higher doses of sulforaphane (Fig. 1) seems to be independent of a G_2-M delay.

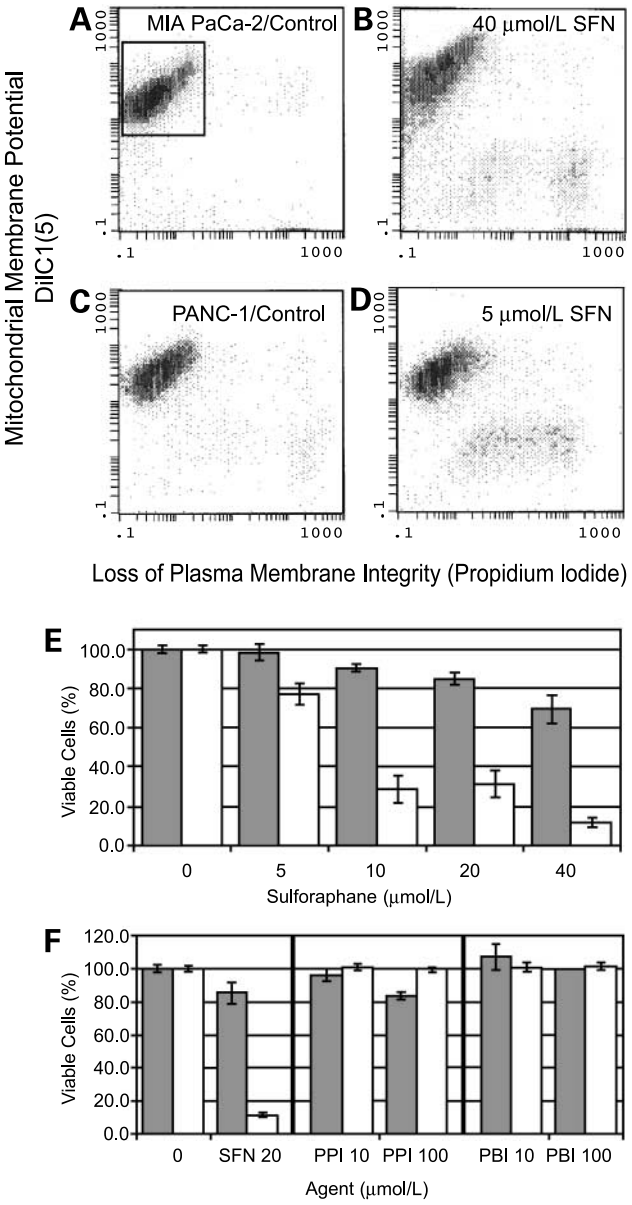

Figure 2. Doses of sulforaphane inducing equal cytotoxicity between MIA PaCa-2 and PANC-1. Correlated dot plots of increasing loss of functional plasma membrane integrity versus MMP labeling for MIA PaCa-2 (**A** and **B**) and PANC-1 (**C** and **D**) cells after 24 hours of sulforaphane incubation. Representative viable cells are identified in *boxed region* (**A**). *Columns,* mean percentage of viable cells from at least three experiments for MIA PaCa-2 (*black bar*) and PANC-1 (*white bar*) cells after isothiocyanate exposures of 24 (**E**) and 48 (**F**) hours; *bars,* SE. *PPI,* phenylpropyl isothiocyanate; *PBI,* phenylbutyl isothiocyanate.

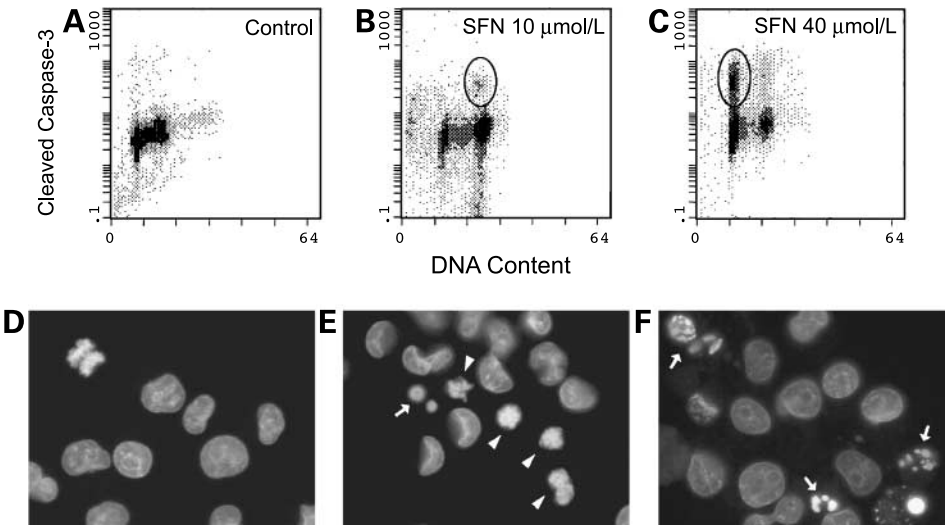

Figure 3. Correlated dot plots of DNA content versus cleaved caspase-3 for untreated MIA PaCa-2 cells (**A**) and cells treated with 10 (**B**) and 40 (**C**) μmol/L sulforaphane for 24 hours. Regions of interest (*circles*) indicate cells with positive anti-cleaved caspase-3. Corresponding images of Hoechst-labeled nuclei show untreated cells (**D**) and sulforaphane-treated cells at 10 (**E**) and 40 (**F**) μmol/L displaying mitotic nuclei (*arrowhead*) and fragmented apoptotic DNA (*arrow*).

MIA PaCa-2 cells treated with 10 μmol/L sulforaphane were not sensitive to UCN-01 (Fig. 6D). UCN-01 abrogates G_2 arrest by the inhibition of Chk1 phosphorylation, permitting the normal progression of cdc25 phosphatase to remove inhibitory phosphate groups from the mitosis-promoting kinase cdc2 (33, 34). The UCN-01-sensitive DNA damage checkpoint seems to be functional in MIA PaCa-2 cells, because γ-irradiated cells arrested at 4C DNA content and irradiated cells followed by 24-hour incubation with UCN-01 failed to arrest (Fig. 6F). The results from more than three independent experiments (Fig. 6G) show that, with 40 μmol/L sulforaphane treatment, cell distribution among the cell cycle phases is not significantly different ($P > 0.2$) from control, untreated cells as compared with values obtained with 10 μmol/L sulforaphane treatment; there is a significant accumulation of cells in G_2-M ($P < 0.001$) and a reduction of cells in G_1 ($P = 0.002$). After UCN-01 treatment, the fraction of 4C in MIA PaCa-2 cells treated simultaneously with irradiation decreased significantly ($P = 0.03$) compared with irradiation alone (Fig. 6H). Although the simultaneous treatment of UCN-01 and sulforaphane showed to a lesser extent a decrease in the fraction of 4C compared with sulforaphane treatment

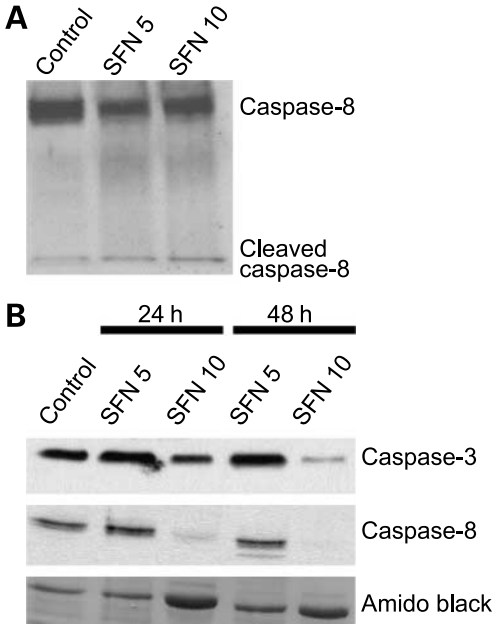

Figure 4. Caspase activation by sulforaphane. By immunoblotting, cleaved caspase-8 was detected after 20 hours of sulforaphane treatment (**A**) and procaspase-8 decreased after 24 hours of treatment (**B**). Activation of caspase-3 as detected by the decrease in procaspase-3 occurred after 48 hours of treatment. The amido black staining is representative of the total protein in each lane.

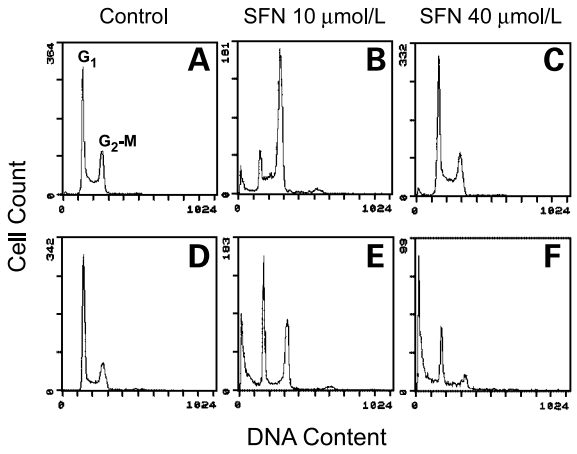

Figure 5. Flow cytometry measurement of single-variable histograms of DNA content. MIA PaCa-2 (*top row*) and PANC-1 (*bottom row*) cells were incubated with sulforaphane for 24 hours at different dose levels: 0 (**A** and **D**), 10 (**B** and **E**), and 40 (**C** and **F**) μmol/L sulforaphane. Accumulation of cells at 4C DNA content was observed when cells were incubated with 10 μmol/L sulforaphane.

alone, the effect was not significant ($P > 0.05$). Thus, molecular mechanisms mediating sulforaphane-induced cell cycle arrest at G_2-M seem to be different from those activated in response to γ radiation.

Mitosis Block by Sulforaphane

To determine the nature of the 4C DNA content accumulation, we evaluated the cell cycle by multiparametric analysis of DNA content, cyclin A, cyclin B1, and pH3. Figure 7 shows that sulforaphane-treated MIA PaCa-2 cells accumulated as a cluster with mitotic levels of pH3 (Fig. 7C, *circle region*), with a mean fold increase of 2.0 ± 0.2 times above untreated cells from three independent experiments ($P = 0.05$). The associated plot of cyclin A versus cyclin B1 (Fig. 7D) of the mitotic cell cluster shows an accumulation of cells that are cyclin A negative and cyclin B1 positive, which is consistent with cells in metaphase (30). This mitotic subpopulation showed a mean fold increase of 2.7 ± 0.3 times above untreated cells ($P < 0.001$) and is consistent with microscopic results (Fig. 3E). A mitotic arrest induced by sulforaphane explains the lack of decreased G_2-M subpopulation when cells treated with sulforaphane were simultaneously incubated with UCN-01 (Fig. 6H). Compared with irradiated cells, which showed an increase in the phosphorylation of cdc2 at Tyr^{15}, a consequence of Chk1 activation leading to a G_2 arrest, this phosphorylation was not observed in sulforaphane-treated cells (Fig. 7G). In addition, sulforaphane was also observed to decrease total cdc2 expression. Cumulatively, these results suggest that sulforaphane deregulates mitosis transit time, thereby inducing a 4C accumulation.

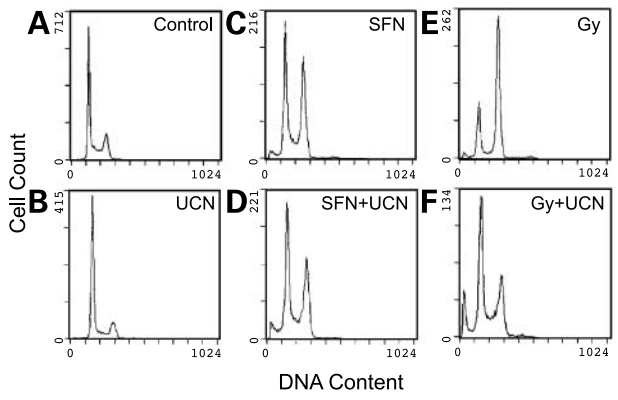

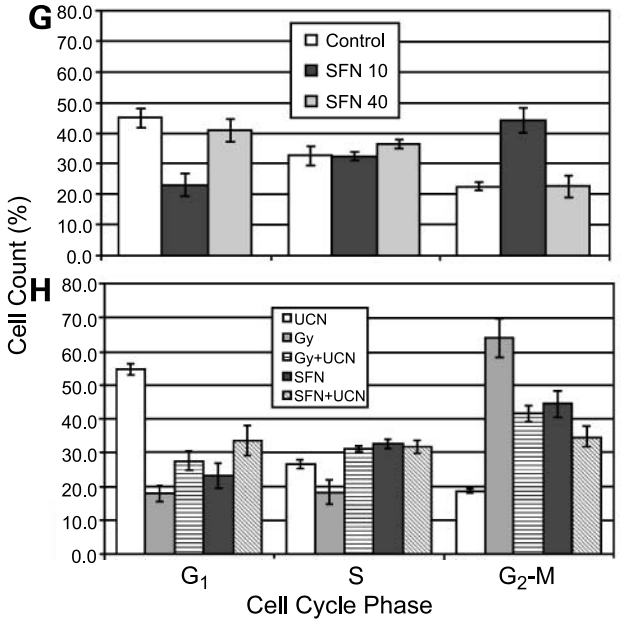

Figure 6. DNA histograms of MIA PaCa-2 cells showing UCN-01 (*UCN*; 100 nmol/L) effect on arrest at 4C DNA content produced by sulforaphane (**C**) compared with γ radiation (*Gy*; **E**) at the end of 24 hours. Combined treatment of cells with UCN-01 and sulforaphane (**D**) showed a less effective and nonsignificant ($P > 0.05$) inhibition at 4C in comparison with a significant inhibition ($P < 0.05$) with UCN-01 and radiation treatment (**F**). *Columns,* mean cell cycle distribution; *bars,* SE (**G** and **H**).

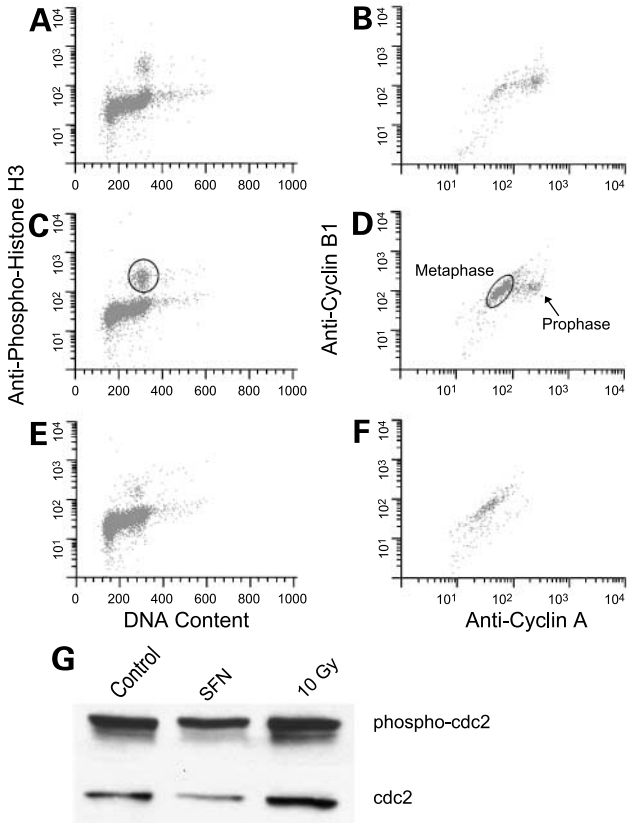

Figure 7. Correlated dot plots of DNA content versus anti-pH3 (**A**, **C**, and **E**) and the corresponding plots of anti – cyclin A versus anti – cyclin B1 (**B**, **D**, and **F**). After 24-hour incubation with 10 μmol/L sulforaphane, MIA PaCa-2 cells accumulated in mitosis (*circle region*, **C**), with a mean fold increase of 2.0 ± 0.2 times above untreated cells (**A**). The corresponding dot plot (**D**) of the mitotic cell cluster shows metaphase accumulation of cells by the expression of maximum levels of cyclin B1 and absence of cyclin A, with a mean fold increase of 2.7 ± 0.3 times above untreated cells (**B**). Cells treated at the higher sulforaphane dose (40 μmol/L) showed a decrease in mitosis (**E** and **F**). By immunoblotting, 24 hours post-treatment shows phospho-cdc2 (Tyr^{15}) and total cdc2 (**G**).

Oxidative Stress and Degree of Cytotoxic Sensitivity to Sulforaphane

As shown in Fig. 8, sulforaphane treatment in MIA PaCa-2 cells caused an increase in cellular reactive oxygen intermediate and GSH in viable MIA PaCa-2 cells (Fig. 8B, box region), whereas PANC-1 cells showed increased reactive oxygen intermediate without an increase in GSH. These results indicate that oxidative stress occurs following sulforaphane treatment. The more sulforaphane-resistant MIA PaCa-2 cells seem to counter this oxidative stress with increased GSH. Sensitivity of PANC-1 cells to sulforaphane was decreased when the apoptosis effectors, caspases, were suppressed and when oxidative stress was reduced (Fig. 9). As shown in Figs. 3 and 4, sulforaphane cytotoxicity is mediated in part by caspase-3 and caspase-8 and consequently may be reduced by incubating simultaneously with a general caspase inhibitor zVAD.fmk. Figure 9B shows the optimal combined doses and duration of continuous incubation for sulforaphane and zVAD.fmk to reduce toxicity of sulforaphane in PANC-1 cells as measured by a functional plasma membrane integrity and MMP. Similarly, the simultaneous incubation of sulforaphane with an antioxidant, *N*-acetyl-L-cysteine, also reduced cell damage (Fig. 9C). The reduction in sulforaphane-induced toxicity by either zVAD.fmk or *N*-acetyl-L-cysteine is consistent with an apoptotic pathway that associates with the generation of reactive oxygen intermediate (35–37) and activation of caspases (38).

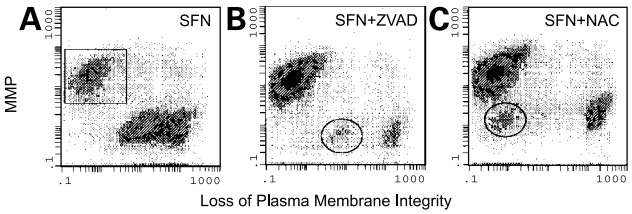

Figure 9. Correlated dot plots of increasing loss of functional plasma membrane integrity versus MMP show that the surviving PANC-1 subpopulation (*boxed region*, **A**) was increased after 24-hour incubation with 10 μmol/L sulforaphane treatment when incubated simultaneously with 100 μmol/L zVAD.fmk (*ZVAD*; **B**) or 2.26 mmol/L *N*-acetyl-L-cysteine (*NAC*; **C**). Cells at intermediate stages of cytotoxicity (*circled regions*) are fewer and more obviously separated from severely damaged cells with the use of zVAD.fmk and *N*-acetyl-L-cysteine.

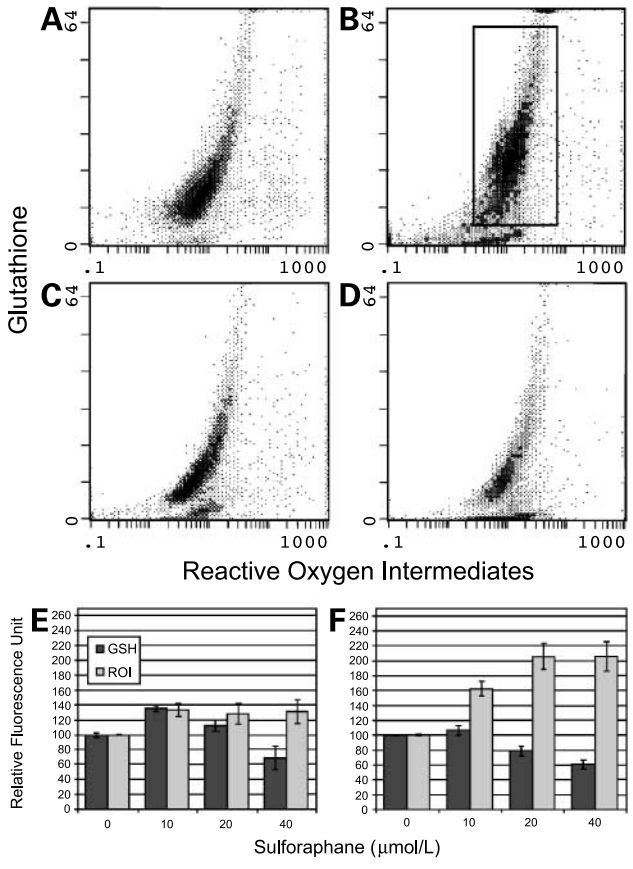

Figure 8. Correlated dot plots of cellular content of reactive oxygen intermediate versus GSH in untreated, control cells compared with 10 μmol/L sulforaphane-treated cells for 24 hours in MIA PaCa-2 (**A** and **B**) and PANC-1 (**C** and **D**), respectively. Summarized flow cytometry analysis of GSH (*black bar*) and reactive oxygen intermediate (*gray bar*) for MIA PaCa-2 (**E**) and PANC-1 (**F**) in viable cells (*box region*, **B**). *Columns,* mean normalized with respect to control; *bars,* SE.

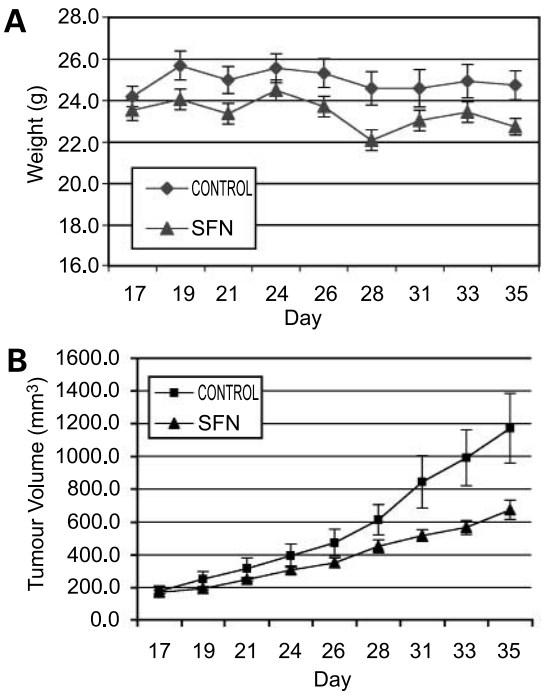

Figure 10. A severe combined immunodeficient mouse tumor xenograft model was used to examine the effects of sulforaphane on s.c. tumor growth. Weights of sulforaphane-treated mice tended to be lower than the PBS-treated, control mice (**A**). The mean tumor volume in sulforaphane-treated mice was significantly less than the control group at the end of 3 weeks ($P = 0.02$).

Effects of Sulforaphane on Growth of PANC-1 Tumor Xenografts

Mice were observed to decrease in activity level when a sulforaphane dose of 500 μmol/kg body weight was given i.p., with death occurring in some animals when the dose was further increased. The given dose, 250 to 400 μmol/kg body weight, was tolerated and similar to doses used by previous studies (7, 39). Animal body weight in sulforaphane-treated group was ~2 g less than controls at the end of 3 weeks ($P = 0.02$). Animals were randomly assigned to treatment groups when tumors had a mean volume of 177 ± 16 mm^3. Growth of the established s.c. tumors in severe combined immunodeficient mice was decreased significantly ($P = 0.02$) when a daily i.p. injection of sulforaphane was given over a period of 3 weeks compared with control PBS-treated animals (Fig. 10). The final mean tumor volume for sulforaphane-treated animals was 696 ± 212 mm^3, 40% less than the control group with a mean of 1,152 ± 496 mm^3.

Discussion

Sulforaphane, a naturally occurring alkyl isothiocyanate, was shown to be a more potent cytotoxic agent than the synthetic analogues phenylpropyl isothiocyanate and phenylbutyl isothiocyanate in MIA PaCa-2 and PANC-1 cells. Cell viability detected by measurement of MMP and plasma membrane integrity indicated that the more lipophilic phenyl substitution did not enhance sulforaphane-induced cytotoxicity, consistent with findings that the cellular uptake of isothiocyanates is predominantly dependent on GSH conjugation reactions promoted by glutathione *S*-transferases (40, 41).

Similar to previous reports, sulforaphane-treated cells showed growth arrest at 4C DNA content with accumulation of cyclin B1 (21, 22). This is consistent with a G_2 and/or M arrest. However, this effect seemed to be independent of a DNA damage Chk1-cdc2 mediated pathway, unlike the G_2 arrest mediated by γ radiation (33), and seemed to be predominantly a metaphase arrest as shown by microscopy and multiparametric cell cycle analysis by flow cytometry. This is similar to the effects of nocodazole and may occur by the disruption of microtubules by sulforaphane (22, 42), whereupon it is expected that the activity of the mitotic spindle checkpoint is maintained and arrest cells in metaphase. Of interest, our findings suggest that cell cycle perturbation and oxidative stress dominate at the low sulforaphane doses, whereas apoptosis and caspase activation dominate at the higher dose. Sulforaphane activated the caspase-8-dependent death receptor pathway, coinciding with the activation of the mitochondrial pathway. Amplification of the death receptor signaling through the mitochondrial pathway has been well described (32). Activation of caspase-8 can cleave the BH3 family member Bid. Truncated Bid then migrates to the mitochondria, leading to the loss of MMP, cytochrome *c* release, and activation of the initiator caspase-9 (43, 44). This is similar to effects of another natural product, combretastatin-A4 (45). The mechanisms of the sulforaphane dose-specific mitosis arrest and their consequences remain unclear in determining the effectiveness of sulforaphane as an anticancer agent.

Our results suggested that the sensitivity of MIA PaCa-2 and PANC-1 cells to sulforaphane was linked to differences in redox regulation response. GSH levels in MIA PaCa-2 cells increased concomitantly with reactive oxygen intermediate at relatively nontoxic doses of sulforaphane, whereas at similar doses a larger subpopulation of PANC-1 cells progressed to irreversible cell damage, with the remaining viable cell subpopulation expressing high reactive oxygen intermediate levels without an increase in cellular GSH. In support of an oxidative stress role in sulforaphane cytotoxicity, simultaneous incubation with the antioxidant *N*-acetyl-L-cysteine reduced toxicity effects of sulforaphane on the highly sulforaphane-sensitive PANC-1 cells. Two apparently distinct effects of isothiocyanates on cellular redox state have been reported. First, isothiocyanates can induce hepatic detoxifying enzymes such as glutathione *S*-transferases as well as GSH levels (46, 47). However, with a few naturally occurring compounds, including sulforaphane, prooxidant effects include the increase in 8-oxo-deoxyguanosine (48). Thus, it seems that the net balance of sulforaphane effects on cells between detoxification and prooxidant pathways could influence the degree of sulforaphane-mediated cytotoxicity as observed for MIA PaCa-2 and PANC-1 cells. The greater sensitivity of PANC-1 cells to the lower doses of sulforaphane was associated with inability to increase GSH levels and might be due to deficient detoxification enzyme induction pathways as reported previously for MCF-7 and HT-29 cells (49). In addition, other oxidative stress–related pathways could be differentially affected including sulforaphane-mediated inhibition of nuclear factor-κB (17).

Recent studies showed that sulforaphane inhibited growth of tumor precursors (50) and growth of tumors in mice models when treatment was started at the time of carcinogen administration (7) and tumor cell implantation (39). We now show that growth of established s.c. PANC-1 tumor xenografts was suppressed at a similar sulforaphane dose. Sulforaphane-induced toxicity in PANC-1 cells was achieved at a treatment dose comparable with the micromolar plasma levels achieved in humans (51, 52). Sulforaphane and related isothiocyanate compounds should therefore be investigated further as anticancer agents in addition to their established effects in cancer prevention.

Acknowledgments

We thank Sue Chow and Kit Frances Tong for their flow cytometry technical assistance. Preliminary work was initiated by grade 13 students from Harbord Collegiate Institute (Sophie Barbier, Katy Dosman, Maureen Wong, and Wei-Jia Zhou) that participated in the Aventis Biotech Challenge 2002.

References

1. Park EJ, Pezzuto JM. Botanicals in cancer chemoprevention. Cancer Metastasis Rev 2002;21:231 – 55.

2. Fahey JW, Zalcmann AT, Talalay P. The chemical diversity and distribution of glucosinolates and isothiocyanates among plants. Phytochemistry 2001;56:5 – 51.

3. Lund E. Non-nutritive bioactive constituents of plants: dietary sources and health benefits of glucosinolates. Int J Vitam Nutr Res 2003;73: 135 – 43.

4. Nagle CM, Purdie DM, Webb PM, Green A, Harvey PW, Bain CJ. Dietary influences on survival after ovarian cancer. Int J Cancer 2003;106:264 – 9.

5. Murillo G, Mehta RG. Cruciferous vegetables and cancer prevention. Nutr Cancer 2001;41:17 – 28.

6. Steinkellner H, Rabot S, Freywald C, et al. Effects of cruciferous vegetables and their constituents on drug metabolizing enzymes involved in the bioactivation of DNA-reactive dietary carcinogens. Mutat Res 2001; 480 – 481:285 – 97.

7. Zhang Y, Kensler TW, Cho CG, Posner GH, Talalay P. Anticarcinogenic activities of sulforaphane and structurally related synthetic norbornyl isothiocyanates. Proc Natl Acad Sci U S A 1994;91:3147 – 50.

8. Kassie F, Uhl M, Rabot S, et al. Chemoprevention of 2-amino-3-methylimidazo[4,5-*f*]quinoline (IQ)-induced colonic and hepatic preneoplastic lesions in the F344 rat by cruciferous vegetables administered simultaneously with the carcinogen. Carcinogenesis 2003;24:255 – 61.

9. Chung FL, Conaway CC, Rao CV, Reddy BS. Chemoprevention of colonic aberrant crypt foci in Fischer rats by sulforaphane and phenethyl isothiocyanate. Carcinogenesis 2000;21:2287 – 91.

10. Fahey JW, Haristoy X, Dolan PM, et al. Sulforaphane inhibits extracellular, intracellular, and antibiotic-resistant strains of *Helicobacter pylori* and prevents benzo[*a*]pyrene-induced stomach tumors. Proc Natl Acad Sci U S A 2002;99:7610 – 5.

11. Hecht SS, Kenney PM, Wang M, Upadhyaya P. Benzyl isothiocyanate: an effective inhibitor of polycyclic aromatic hydrocarbon tumorigenesis in A/J mouse lung. Cancer Lett 2002;187:87 – 94.

12. Lampe JW, Peterson S. *Brassica,* biotransformation and cancer risk: genetic polymorphisms alter the preventive effects of cruciferous vegetables. J Nutr 2002;132:2991 – 4.

13. Brooks JD, Paton VG, Vidanes G. Potent induction of phase 2 enzymes in human prostate cells by sulforaphane. Cancer Epidemiol Biomarkers Prev 2001;10:949 – 54.

14. Chen YR, Wang W, Kong AN, Tan TH. Molecular mechanisms of c-Jun N-terminal kinase-mediated apoptosis induced by anticarcinogenic isothiocyanates. J Biol Chem 1998;273:1769 – 75.

15. Xiao D, Singh SV. Phenethyl isothiocyanate-induced apoptosis in p53-deficient PC-3 human prostate cancer cell line is mediated by extracellular signal-regulated kinases. Cancer Res 2002;62:3615 – 9.

16. Zhu CY, Loft S. Effect of chemopreventive compounds from *Brassica* vegetables on NAD(P)H:quinone reductase and induction of DNA strand breaks in murine hepa1c1c7 cells. Food Chem Toxicol 2003;41:455 – 62.

17. Heiss E, Herhaus C, Klimo K, Bartsch H, Gerhauser C. Nuclear factor κB is a molecular target for sulforaphane-mediated anti-inflammatory mechanisms. J Biol Chem 2001;276:32008 – 15.

18. Gao X, Dinkova-Kostova AT, Talalay P. Powerful and prolonged protection of human retinal pigment epithelial cells, keratinocytes, and mouse leukemia cells against oxidative damage: the indirect antioxidant effects of sulforaphane. Proc Natl Acad Sci U S A 2001;98:15221 – 6.

19. Hasegawa T, Nishino H, Iwashima A. Isothiocyanates inhibit cell cycle progression of HeLa cells at G_2-M phase. Anticancer Drugs 1993;4: 273 – 9.

20. Fimognari C, Nusse M, Cesari R, Iori R, Cantelli-Forti G, Hrelia P. Growth inhibition, cell-cycle arrest and apoptosis in human T-cell leukemia by the isothiocyanate sulforaphane. Carcinogenesis 2002;23:581 – 6.

21. Gamet-Payrastre L, Li P, Lumeau S, et al. Sulforaphane, a naturally occurring isothiocyanate, induces cell cycle arrest and apoptosis in HT29 human colon cancer cells. Cancer Res 2000;60:1426 – 33.

22. Xiao D, Srivastava SK, Lew KL, et al. Allyl isothiocyanate, a constituent of cruciferous vegetables, inhibits proliferation of human prostate cancer cells by causing G_2-M arrest and inducing apoptosis. Carcinogenesis 2003; 24:891 – 7.

23. DiPaola RS. To arrest or not to G(2)-M cell-cycle arrest. Commentary re: A.K. Tyagi et al., Silibinin strongly synergizes human prostate carcinoma DU145 cells to doxorubicin-induced growth inhibition, G(2)-M arrest, and apoptosis. Clin Cancer Res 2002;8:3512 – 9.

24. Butz J, Wickstrom E, Edwards J. Characterization of mutations and loss of heterozygosity of p53 and K-*ras*2 in pancreatic cancer cell lines by immobilized polymerase chain reaction. BMC Biotechnol 2003;3:11.

25. Mohiuddin M, Chendil D, Dey S, Alcock RA, Regine W, Ahmed MM. Influence of p53 status on radiation and 5-flourouracil synergy in pancreatic cancer cells. Anticancer Res 2002;22:825 – 30.

26. Alcock RA, Dey S, Chendil D, et al. Farnesyltransferase inhibitor (L-744,832) restores TGF-β type II receptor expression and enhances radiation sensitivity in K-*ras* mutant pancreatic cancer cell line MIA PaCa-2. Oncogene 2002;21:7883 – 90.

27. Keck AS, Staack R, Jeffery EH. The cruciferous nitrile crambene has bioactivity similar to sulforaphane when administered to Fischer 344 rats but is far less potent in cell culture. Nutr Cancer 2002;42:233 – 40.

28. Ng SSW, Tsao MS, Chow S, Hedley DW. Inhibition of phosphatidylinositide 3-kinase enhances gemcitabine-induced apoptosis in human pancreatic cancer cells. Cancer Res 2000;60:5451 – 5.

29. Backway KL, McCulloch EA, Chow S, Hedley DW. Relationships between the mitochondrial permeability transition and oxidative stress during ara-C toxicity. Cancer Res 1997;57:2446 – 51.

30. Soni DV, Jacobberger JW. Inhibition of Cdk1 by alsterpaullone and thioflavopiridol correlates with increased transit time from mid G(2) through prophase. Cell Cycle 2004:3.

31. Gleave M, Hsieh JT, Gao CA, von Eschenbach AC, Chung LW. Acceleration of human prostate cancer growth *in vivo* by factors produced by prostate and bone fibroblasts. Cancer Res 1991;51:3753 – 61.

32. Fumarola C, Guidotti GG. Stress-induced apoptosis: toward a symmetry with receptor-mediated cell death. Apoptosis 2004;9:77 – 82.

33. Hu B, Zhou XY, Wang X, Zeng ZC, Iliakis G, Wang Y. The radioresistance to killing of A1-5 cells derives from activation of the Chk1 pathway. J Biol Chem 2001;276:17693 – 8.

34. Feijoo C, Hall-Jackson C, Wu R, et al. Activation of mammalian Chk1 during DNA replication arrest: a role for Chk1 in the intra-S phase checkpoint monitoring replication origin firing. J Cell Biol 2001;154: 913 – 23.

35. Lambert C, Thews O, Biesalski HK, Vaupel P, Kelleher DK, Frank J. 2-Methoxyestradiol enhances reactive oxygen species formation and increases the efficacy of oxygen radical generating tumor treatment. Eur J Med Res 2002;7:404 – 14.

36. Gordon J, Wu C-H, Rastegar M, Safa A. β_2-Microglobulin induces caspase-dependent apoptosis in the CCRF-HSB-2 human leukemia cell line independently of the caspase-3, -8 and -9 pathways but through increased reactive oxygen species. Int J Cancer 2003;103:316 – 27.

37. Sasaki M, Kobayashi D, Watanabe N. Augmented Adriamycin sensitivity in cells transduced with an antisense tumor necrosis factor gene is mediated by caspase-3 downstream from reactive oxygen species. Jpn J Cancer Res 2001;92:983 – 8.

38. Kim SG, Jong HS, Kim TY, et al. Transforming growth factor-β 1 induces apoptosis through Fas ligand-independent activation of the Fas death pathway in human gastric SNU-620 carcinoma cells. Mol Biol Cell 2004;15:420 – 34.

39. Singh AV, Xiao D, Lew KL, Dhir R, Singh SV. Sulforaphane induces caspase-mediated apoptosis in cultured PC-3 human prostate cancer cells and retards growth of PC-3 xenografts *in vivo.* Carcinogenesis 2004;25: 83 – 90.

40. Zhang Y. Molecular mechanism of rapid cellular accumulation of anticarcinogenic isothiocyanates. Carcinogenesis 2001;22:425 – 31.

41. Jiao D, Eklind KI, Choi CI, Desai DH, Amin SG, Chung FL. Structure-activity relationships of isothiocyanates as mechanism-based inhibitors of 4-(methylnitrosamino)-1-(3-pyridyl)-1-butanone-induced lung tumorigenesis in A/J mice. Cancer Res 1994;54:4327 – 33.

42. Jackson SJ, Singletary KW. Sulforaphane: a naturally occurring mammary carcinoma mitotic inhibitor which disrupts tubulin polymerization. Carcinogenesis 2004;25:219 – 27.

43. Gingras D, Gendron M, Boivin D, Moghrabi A, Theoret Y, Beliveau R. Induction of medulloblastoma cell apoptosis by sulforaphane, a dietary anticarcinogen from *Brassica* vegetables. Cancer Lett 2004;203: 35 – 43.

44. Nabhan C, Gajria D, Krett NL, Gandhi V, Ghias K, Rosen ST. Caspase activation is required for gemcitabine activity in multiple myeloma cell lines. Mol Cancer Ther 2002;1:1221 – 7.

45. Nabha SM, Mohammad RM, Dandashi MH, et al. Combretastatin-A4 prodrug induces mitotic catastrophe in chronic lymphocytic leukemia cell line independent of caspase activation and poly(ADP-ribose) polymerase cleavage. Clin Cancer Res 2002;8:2735 – 41.

46. Ye L, Zhang Y. Total intracellular accumulation levels of dietary isothiocyanates determine their activity in elevation of cellular glutathione and induction of phase 2 detoxification enzymes. Carcinogenesis 2001; 22:1987 – 92.

47. Basten GP, Bao Y, Williamson G. Sulforaphane and its glutathione conjugate but not sulforaphane nitrile induce UDP-glucuronosyl transferase (UGT1A1) and glutathione transferase (GSTA1) in cultured cells. Carcinogenesis 2002;23:1399 – 404.

48. Srinivasan P, Vadhanam MV, Arif JM, Gupta RC. A rapid screening assay for antioxidant potential of natural and synthetic agents *in vitro.* Int J Oncol 2002;20:983 – 6.

49. Jiang ZQ, Chen C, Yang B, Hebbar V, Kong AN. Differential responses from seven mammalian cell lines to the treatments of detoxifying enzyme inducers. Life Sci 2003;72:2243 – 53.

50. Smith TK, Mithen R, Johnson IT. Effects of *Brassica* vegetable juice on the induction of apoptosis and aberrant crypt foci in rat colonic mucosal crypts *in vivo*. Carcinogenesis 2003;24:491 – 5.

51. Ye L, Dinkova-Kostova AT, Wade KL, Zhang Y, Shapiro TA, Talalay P. Quantitative determination of dithiocarbamates in human plasma, serum, erythrocytes and urine: pharmacokinetics of broccoli sprout isothiocyanates in humans. Clin Chim Acta 2002;316:43 – 53.

52. Shapiro TA, Fahey JW, Wade KL, Stephenson KK, Talalay P. Chemoprotective glucosinolates and isothiocyanates of broccoli sprouts: metabolism and excretion in humans. Cancer Epidemiol Biomarkers Prev 2001;10:501 – 8.

Molecular Cancer Therapeutics

The dietary isothiocyanate sulforaphane targets pathways of apoptosis, cell cycle arrest, and oxidative stress in human pancreatic cancer cells and inhibits tumor growth in severe combined immunodeficient mice

Nhu-An Pham, James W. Jacobberger, Aaron D. Schimmer, et al.

Mol Cancer Ther 2004;3:1239-1248.